Ocean Science
Discussions

Open Access

The open boundary equation

D. Diederen[1], H. H. G. Savenije[1], and M. Toffolon[2]

[1]Department of Water Management, Delft University of Technology, Delft, the Netherlands
[2]Department of Civil, Environmental and Mechanical Engineering, University of Trento, Trento, Italy

Correspondence to: H. H. G. Savenije (h.h.g.savenije@tudelft.nl)

Title Page

Abstract	Introduction
Conclusions	References
Tables	Figures

Back | Close

Full Screen / Esc

Printer-friendly Version

Interactive Discussion

Abstract

We present a new equation describing the hydrodynamics in infinitely long tidal channels (i.e., no reflection) under the influence of oceanic forcing. The proposed equation is a simple relationship between partial derivatives of water level and velocity. It is formally derived for a progressive wave in a frictionless, prismatic, tidal channel with a horizontal bed. Assessment of a large number of numerical simulations, where an open boundary condition is posed at a certain distance landward, suggests that it can also be considered accurate in the more natural case of converging estuaries with nonlinear friction and a bed slope. The equation follows from the open boundary condition and is therefore a part of the problem formulation for an infinite tidal channel. This finding provides a practical tool for evaluating tidal wave dynamics, by reconstructing the temporal variation of the velocity based on local observations of the water level, providing a fully local open boundary condition and allowing for local friction calibration.

1 Introduction

The behavior of tidal waves in natural estuaries has been the subject of numerous studies with different degrees of complexity. For rapid assessment, the tidal dynamics in these estuaries may be described as one-dimensional, whereby the standard Saint-Venant shallow water equations are used as the governing equations. For long waves, one-dimensional descriptions are appropriate in long water bodies, where the length is much larger than the width.

De Saint-Venant (1871) formulated the governing equations in the Eulerian reference frame, which has the advantage that the reference frame does not move. An exact analytical solution of such equations is not available, so various approximations have been proposed. Perturbation methods (e.g., Hunt, 1964; Jay, 1991; Friedrichs and Aubrey, 1994) are particularly useful to this aim, since they can capture the approximate dynamics conceptually. The Eulerian reference frame is also convenient for numerical

methods, where a grid has to be defined and a non-moving grid has a clear advantage. These numerical approximations may not provide conceptual relations between parameters, but they do permit the analysis of complex geometries and retain the full nonlinear behavior. In addition to the Eulerian perspective, we may rewrite the governing equations in the Lagrangean reference frame, where an observer moves with the speed of the water particle. This provides additional insight in the wave character and allows for a different approximate analytical approach (Savenije, 2005, 2012). There the structure of the solution is assumed a priori in the form of a sinusoidal function, but nonlinear terms in advection and friction can be retained. A third perspective is that of the "Riemann invariants" (Riemann, 1859), or "method of characteristics", where the observer moves with the propagation speed of disturbances. For long estuaries, this "celerity" is a main parameter in most analytical approximate solutions. Moreover, the Riemann perspective provides approximations for open boundaries.

Analytical descriptions can easily treat infinitely long channels, whereas numerical models require an artificial "open" boundary condition (Orlanski, 1976), where the propagating wave exits a limited domain unaffected. Such a boundary can also be referred to as "absorbing" (Engquist and Majda, 1977), since waves that hit this boundary are absorbed instead of reflected (as would be the case when they hit a closed boundary), or as "non-reflective" (Keller and Voli, 1989). Perfectly functioning open boundaries in numerical tidal hydraulics have yet to be defined, so a small part of the wave is always reflected. Yet, a perfect open boundary condition is required for long estuaries where the examined domain is limited. Using an open boundary, the domain can be split into multiple reaches to be solved subsequently (e.g., Keller and Voli, 1989; Toffolon and Savenije, 2011). Theoretically, with this splitting method the domain can be divided into an infinite number of reaches. Since the open boundary condition is applied at each location in the domain, this condition becomes an equation. Here we present the "open boundary equation".

The Riemann invariants suggest that any solution for sub-critical flow is composed of pieces of information that are advected in positive and negative direction. This also

applies for a wave which physically seems to move only in one direction. However, the tidal wave character is usually described as either a single incident wave or the super-position of an incident and a reflected wave. This superposition finds its origin in linear wave theory, specifically for frictionless, prismatic, horizontal channels with a closed landward boundary, where the incident wave and its reflection have the same strength. In that basic scenario a phase lag of 90° can be observed between the water depth and the velocity. Interestingly, a phase lag can also be observed in long, converging estuaries, where there is no such closed boundary. The terminology to describe the tidal wave character in such natural estuaries appears to be subject to debate. Is the phase lag, which is observed in long converging estuaries, similar to the phase lag that is caused by the reflection of a closed landward boundary? In other words, should we call it "reflection"? Hunt (1964) warned that the use of the classical terms "progressive wave" and "standing wave" to a frictional situation should be treated with "considerable caution". He prefers the description by a single wave over the description by a super-imposed incident and reflected wave, and he calls this single wave standing when it shows a phase lag. Jay (1991) argued that the use of descriptions like "progressive" and "standing" should not be used in convergent estuaries, for two reasons. First, fric-tion and convergence play a large role in estuaries and so even perfect reflection by a barrier would lead to a standing wave only at the point of reflection. Second, any phase lag from 0 to 90° can occur for a single incident wave. Friedrichs and Aubrey (1994) found that a single incident wave in a converging estuary can have a 90° phase lag, but can have a celerity close to that of a frictionless progressive wave. Savenije et al. (2008) described that a wave with a mixed character occurs in convergent estu-aries and attributes this to convergence and friction. They also showed that the wave character depends on the phase speed, which in turn depends on the phase lag. Nev-ertheless, all these authors concluded that the "apparent reflection" in an estuary is different from the "classical reflection" produced by a closed boundary.

In this paper we consider a long, exponentially converging estuary, where the in-fluence of the landward boundary condition is negligible so that the reflected wave is

Open boundary equation

D. Diederen et al.

Title Page

Abstract | Introduction

Conclusions | References

Tables | Figures

◄ | ►

◄ | ►

Back | Close

Full Screen / Esc

Printer-friendly Version

Interactive Discussion

negligible. This is quite a common case in real alluvial estuaries, and can be approximated as an "infinitely long" channel, where the reflected wave is non-existent. Here we derive a new, additional equation, which appears to be a part of the problem formulation. First we derive the equation exactly in a frictionless, prismatic, horizontal channel in Sect. 2.3, then we test the performance of the equation in numerical simulations with friction and convergence in Sect. 3. We discuss the origin of the new equation in Sect. 4. Then we present a new method to look at the tidal wave character in Sect. 5. Finally, we propose applications of the new equation for hydrological and hydraulic purposes in Sect. 6.

2 Formulation of the problem

2.1 Eulerian perspective

The Saint-Venant equations are generally used to analyze water flow in channels and estuaries. Together the mass balance (Eq. 1) and momentum balance (Eq. 2) describe the movement of the water, where, within the Eulerian perspective, the subscripts refer to partial derivatives in space and time. These equations are useful for an observer at a given location along the channel,

$$h_t + uh_x + hu_x - \beta uh = 0, \tag{1}$$
$$u_t + uu_x + g\zeta_x + W = 0, \tag{2}$$
$$h = \zeta - Z, \qquad \beta = -\frac{B_x}{B}, \tag{3}$$

where x is the longitudinal coordinate (positive landward), t is the time, g is the acceleration due to gravity, $u(x,t)$ is the cross-sectional average flow velocity, $h(x,t)$ is the water depth, $\zeta(x,t)$ is the water level, $Z(x)$ is the bed level, $B(x)$ is the width and $W(x,t)$ is the frictional term.

2.2 Riemann perspective

The observer can also choose to move with the wave, for which rewriting Eqs. (1) and (2) into the Riemann perspective of invariants is convenient,

$$R_{1,t} + (u + c)R_{1,x} = \beta u c - gZ_x - W \,, \tag{4}$$
$$R_{2,t} + (u - c)R_{2,x} = -\beta u c - gZ_x - W \,, \tag{5}$$

where the Riemann invariants are defined by

$$R_1 = u + 2c \,, \qquad R_2 = u - 2c \,, \tag{6}$$

and $c = \sqrt{gh}$ is the long wave celerity for small amplitudes.

In this paper we restrict our focus on sub-critical flow since this is the typical case in tidal flows. Hence, the Froude number $|u|/c < 1$, so that one invariant is advected in the positive direction and the other in the negative direction, as can be seen in Eqs. (4) and (5).

2.3 Analytical derivation for a "perfect channel"

The first step towards the open boundary equation is to derive it analytically for a "perfect channel", which we specify as an infinitely long, prismatic channel where convergence and friction are zero and the bed is horizontal, hence $B_x = 0$, $W = 0$ and $h_x = \zeta_x$. The basic equations in Eulerian form (Eqs. 1 and 2), and in Riemann form (Eqs. 4 and 5) then reduce to:

$$h_t + uh_x + hu_x = 0 \,, \tag{7}$$
$$u_t + uu_x + gh_x = 0 \,, \tag{8}$$
$$R_{1,t} + (u + c)R_{1,x} = 0 \,, \tag{9}$$
$$R_{2,t} + (u - c)R_{2,x} = 0 \,. \tag{10}$$

We assume an infinite domain from $x = 0$ to $x = \infty$ to avoid reflection from a closed landward boundary. We put a forcing boundary condition seaward. As initial condition, we impose a constant $R_2(x,0) = C$, where starting with a constant velocity (e.g. $u(x,0) = 0$) and a constant water level (e.g. $\zeta(x,0) = 0$) is the easiest option.

In sub-critical flow the two invariants R_1 and R_2 are transported in opposite direction. Tracking the seaward propagating invariant $R_2(x_2,t_2)$ back in time from a location x_2 within the domain, eventually the trajectory will lead back to an initial condition $R_2(x_1,0)$. This arrival point x_1 will also be in the infinite domain, because in sub-critical flow the celerity $(u - c)$ of R_2 is negative, so that $x_1 > x_2$.

If we integrate Eq. (10) along the pathway of R_2 from x_1 to x_2,

$$R_2(x_2,t_2) = R_2(x_1,0) + \int_0^{t_2} \frac{dR_2}{dt} dt, \tag{11}$$

where the operator $d/dt = \partial/\partial t + (u - c)\partial/\partial x$ represents the full Riemann derivative for R_2, we find that $R_2(x_2,t_2) = R_2(x_1,0)$ (hence the term invariant). Since x_2 can be any location in the domain and t_2 can be any time, the initial condition $R_2(x,0) = C$ in an infinitely long channel with sub-critical flow leads to $R_2(x,t) = C$.

This means that if we differentiate Eq. (6b) in space and in time, we obtain

$$R_{2,x} = 0, \tag{12}$$
$$R_{2,t} = 0, \tag{13}$$

so that

$$\sqrt{h}u_x = \sqrt{g}h_x, \tag{14}$$
$$\sqrt{h}u_t = \sqrt{g}h_t. \tag{15}$$

By combining Eq. (14) with Eq. (15) we obtain

$$h_t u_x = u_t h_x, \tag{16}$$

and

$$hu_t u_x = gh_t h_x. \tag{17}$$

Moreover, from the Lagrangean perspective we find

$$\frac{Dh}{Dt}u_x = \frac{Du}{Dt}h_x, \tag{18}$$

$$\sqrt{h}\frac{Du}{Dt} = \sqrt{g}\frac{Dh}{Dt}, \tag{19}$$

where the operator $D/Dt = \partial/\partial t + u\,\partial/\partial x$ represents the full Lagrangean derivative. From the Riemann perspective we find

$$R_{1,t}R_{2,x} = R_{2,t}R_{1,x}, \tag{20}$$

$$R_{1,t}R_{2,x} = -R_{2,t}R_{1,x}, \tag{21}$$

which seem to indicate a contradiction. However, this is not the case since one of the invariants is constant in space and time, so the contradiction is removed by triviality, as zero is zero.

These equations all contain the same latent information for a "perfect channel", i.e. if one applies, so do the others. What is enclosed in these equations is the infinite domain, which implies they are also valid for a simulation with a finite domain and an open landward boundary condition. We further discuss this in Sect. 4.

Since for a horizontal bed $\zeta_x = h_x$, we rewrite Eq. (16) to

$$\zeta_t u_x = u_t \zeta_x, \tag{22}$$

which we call "the open boundary equation". This way the latent information is expressed independent of the geometry. Examples to derive Eq. (22) from simple analytical approximations are presented in Appendix A. Could it be that Eq. (22) also applies more generally, in estuaries with friction, convergence and a bed slope?

3 Testing the open boundary equation

3.1 Frictional and convergent estuaries

Man-made channels may be straight, but natural estuaries usually converge in land-ward direction, so that $\beta \neq 0$ in the mass balance (Eq. 1). The change of width of alluvial estuaries can be well described by an exponential function (e.g., Savenije, 2012),

$$B = B_\infty + (B_0 - B_\infty)\exp\left(-\frac{x}{b}\right), \tag{23}$$

where B_0 is the width at the mouth of the estuary, B_∞ is the asymptotic value of the width and b is the convergence length of the width. Additionally, an exponentially converging bed level is assumed, with

$$Z = -\overline{h}_0 \exp\left(-\frac{x}{d}\right), \tag{24}$$

where $\overline{h}_0$ is the average depth at the mouth and d is the convergence length of the bed. Since there is a bed slope: $h_x = \zeta_x - Z_x$. As in reality there will always be friction in the momentum balance (Eq. 2), we apply the empirical formula

$$W = g\frac{u|u|}{K^2 h^{4/3}}, \tag{25}$$

where K is the Strickler coefficient.

So what happens with Eq. (22) when there is convergence of width, a bed slope and friction? These terms do not appear in Eq. (22), so might it still hold?

We assume that Eq. (22) holds in frictional, convergent estuaries, in order to see if we can reason back analytically to confirm that it actually holds. In Sect. 2.3, where a "perfect channel" was analyzed, derivation of the negative invariant R_2 in space and time led to the two ordinary differential Eqs. (14) and (15). We can obtain similar ordinary

differential equations by combining Eqs. (1), (2) and (22), which yields the following two equations:

$$h u_x{}^2 - (Z_x + \beta h) u u_x = g \zeta_x{}^2 + W \zeta_x, \qquad (26)$$

$$hu_t{}^2 + \left(hW + \beta h u^2 + u^2 Z_x \right) u_t = g h_t{}^2 - (W + \beta g h + g Z_x) u h_t. \qquad (27)$$

Since these ordinary differential equations are highly nonlinear, we cannot simply integrate back to the negative invariant R_2, which would be the inverse route as applied in Sect. 2.3. Therefore, we think it is not possible to check for correctness analytically, so we resort to numerical testing.

3.2 Numerical modeling

Numerical results cannot prove analytical equations to be correct, as they are single realizations that cannot be used to extrapolate general results. Moreover, they are approximations that contain numerical errors. However, the validity of a given relationship can be tested by running a large number of numerical simulations: if the results are not contradicting it, the argument supporting its validity becomes stronger as the range of the conditions tested becomes wider. Therefore, we use numerical experiments to estimate the difference between the left hand and the right hand sides of the equations, and check if they differ within acceptable thresholds. If so, they can be tested for practical applications. Moreover, if the agreement appears to be consistent, further attempts to find formal proof could also be encouraged.

Simulations are performed by solving Eqs. (1) and (2) with the numerical model described in Toffolon et al. (2006). A sinusoidal periodic oscillation of the water level is imposed at the seaward boundary with an amplitude η and a period $T = 12.41$ h corresponding to a dominant M_2 tide. The width at the mouth B_0 is fixed at 10 km and the asymptotic value B_∞ is fixed at 10 m. The length of the domain L is chosen as twice the wavelength $L_0 = c_0 T$, where $c_0 = \sqrt{g \overline{h}_0}$ is the linearized tidal wave celerity in "perfect

channels" and T is the tidal period. Starting from the initial conditions $\zeta(x,0) = 0$ and $u(x,0) = 0$, the simulations last until an approximate periodic equilibrium is reached.

The governing equations (Eqs. 1 and 2) are evaluated, so we can choose to check Eqs. (22), (26) or (27). We start with time series analysis of a single simulation for Eq. (26) in Fig. 2, which contains friction W, convergence β and bed slope Z_x. In a single wave period, two peaks occur in the squared terms, where the larger peak is the steeper wave front and the smaller peak is the rear. The size of these peaks is mostly influenced by the amplitude-to-depth ratio, which in this case has been chosen small. This way it can easily be observed that good agreement of the left hand side of Eq. (26) and the right hand side can be found when the terms containing the width convergence, the friction and the bed slope are not negligible in size compared to the larger squared terms.

Figure 3 illustrates the longitudinal variation of the Pearson correlation coefficient ρ, which correlates time series of the left hand side of Eq. (22) and the right hand side. It suggests that the validity of the proposed equation is asymptotically reached, with a clear effect of the seaward boundary, where a higher amplitude-to-depth ratio starts with a lower correlation, but converges faster. It should be observed that the imposed seaward boundary is not a naturally occurring relationship between water level and flow, and therefore is not consistent with Eq. (22). The disturbance created by the seaward boundary condition requires a certain length for the tidal wave to adjust. There also is a clear effect of the landward boundary, as a result of the weakly reflective numerical boundary condition. For horizontal estuaries, this effect disappears quickly in seaward direction due to channel convergence and friction, but a bed slope severely increases the length of this effect.

The positive result for Eq. (22) in a single estuary does not mean it applies in general. Therefore, we have analyzed the effect of friction, convergence and amplitude-to-depth ratio for a large number of different cases by extracting values in a wide range of the parameters. In order to define reasonable values for different estuaries, we introduce

three dimensionless parameters (Toffolon et al., 2006)

$$\alpha = \frac{\eta}{\overline{h}_0}, \quad \gamma_b = \frac{c_0}{b\,\varpi}, \quad \gamma_d = \frac{c_0}{d\,\varpi}, \tag{28}$$

where η and $\overline{h}_0$ are the reference values at the mouth of the estuary and $\varpi = 2\pi T^{-1}$ is the tidal frequency. For each simulation, a random value of the following parameters has been selected from a uniform distribution in the range defined in Table 1. We note that $\overline{h}_0$ is selected in a dimensional range because it provides the physical size of the estuary, and K as well to avoid unrealistic friction.

The result of several typical cases is shown in Fig. 4. Each point represents a calculation at a certain location and time in the estuary of Eq. (22), which has been made dimensionless by dividing by the scale factor $F_{sc} = \eta^2/(\overline{h}_0 T^2)$ to get points of as many different scenarios as possible in a single figure. Small values of Eq. (22) demonstrate considerable scatter, which may be explained by numerical errors, which are relatively large in this range. Large values give an almost perfect agreement.

4 Interpretation of the new equation

4.1 Simulating an open boundary condition

The objective of an "open" or "absorbing" boundary condition in wave theory is to not create reflection. It is appropriately used when posed far enough from a reflecting physical boundary, since otherwise physical reflection should be accounted for. It can be applied in sub-critical flow, where information travels in two directions: positive (R_1) and negative (R_2).

The length of influence of a reflection depends on several parameters, such as friction, convergence, bed slope and amplitude-to-depth ratio. Mathematically, the only way to be certain that there is no reflection is to simulate an infinitely long channel. In

fact this means that the perfect open boundary condition implies that behind it there is an infinitely long channel.

As shown in Fig. 5, in sub-critical flow the solution can depend on: (i) two boundary conditions (point A); (ii) one boundary value and one initial condition (B, C); or (iii) two initial conditions (D). An open boundary, which is represented by the dash-dot line, turns point A into the second option, and point B into the third option through the extension by the dashed lines.

A local open boundary should mimic the information that otherwise would have come from outside the domain. This is simple and well known for a "perfect channel", whereas initial condition outside the domain R_2 is assumed to be constant and where the value of R_2 does not change along its trajectory (as Eq. 10 implies).

However, it is more difficult to reproduce this condition when additional terms like friction, convergence and bed slope are accounted for as in Eq. (5), whereby the values of the invariants change along their trajectories. In other words, then the term "invariants" is no longer appropriate. The changes in value of R_2 along its trajectory and the trajectory itself depend on the local solution of the water depth h and the velocity u, which cannot be calculated on a part of the trajectory (see the dashed lines in Fig. 5), since that part lies outside the domain. Approximations for open boundaries exist for linearized cases (e.g., Engquist and Majda, 1977) or with non-local formulas (e.g., Keller and Voli, 1989).

4.2 Domain-splitting and internal open boundaries

The simulation of a progressive wave in a computational domain can be divided into sub-domains with internal boundary conditions (Keller and Voli, 1989; Toffolon and Savenije, 2011). The sub-domains can be explicitly solved from left to right if the reflected wave does not exist or can be neglected, so that the landward boundary can be seen as open. Hence, the solution at the open boundary of each sub-domain can be used as the seaward boundary condition for the next sub-domain (see Fig. 6). Sim-

ulation with sub-domains should result in the same physical simulation as when using a single domain.

Let us assume that it is generally possible to define such internal open boundaries for estuaries with friction, convergence and a bed slope (and not merely for a "perfect channel"). Each internal open boundary should then contain the same information in the sense that behind the boundary lies an infinitely long channel with the same friction and convergence properties as in the entire domain. This implies that the total domain can be described by an infinite number of subdomains, and therefore by an infinite number of open boundaries (see Fig. 6), all containing the same physical information. The boundary condition, which applies locally, becomes an additional equation valid at each location in the domain. This means that instead of an open boundary condition, the additional Eq. (22) is part of the problem formulation for an infinite channel. Similarly, an additional equation (see (A12) in the Appendix) was applied by Savenije (2012), where he assumed a proportional damping equation to represent the open boundary equation, valid for long open boundary estuaries.

5   Wave character in convergent estuaries

5.1   Phase lag and reflection

Descriptions of waves as "progressive" or "standing" originate from the analysis of channels which are frictionless, prismatic and horizontal. The primary indicator for these classifications is the phase lag between the water height h and the velocity u, which is 0° for a perfect progressive wave and 90° for a perfect standing wave. In Sect. 2.3 such a "perfect channel" was analyzed, with an infinite length and therefore no physical, closed boundary. The absence of reflection allows a progressive wave to occur. If such a channel has a closed boundary, full reflection will cause a standing wave to occur.

Clearly, reflection leads to a phase lag. However, we also expect a phase lag in a converging estuary with an open boundary. Moreover, friction and bed slope will influence the phase lag. If we observe a phase lag, does this mean there is reflection?

5.2 Lagrangean analysis

When we follow a fixed volume that moves through a horizontal channel with a varying width, it is compressed in both longitudinal and lateral direction. Dictated by the mass balance, the variation of the water depth follows from this compression. To be able to follow a particle with a given volume of water in a converging estuary, Eq. (1) is rewritten in the Lagrangean perspective (Savenije, 1992),

$$\frac{1}{h}\frac{Dh}{Dt} + u_x - \beta u = 0 \,. \tag{29}$$

This equation shows that the relative change of the depth of a water volume is determined by the velocity gradient and the convergence. When tracking this fixed volume, the displacement S can be obtained by

$$S = \int_0^t u Dt \,. \tag{30}$$

The general solution of the mass balance (Eq. 29) for a converging estuary is

$$h = h_i \exp\left(\int -u_x \, Dt\right) \exp\left(\int \beta u \, Dt\right), \tag{31}$$

where h_i is the initial condition. The first integral represents the longitudinal compression due to the velocity gradient and the second integral the lateral compression due to convergence. Combining Eqs. (30) and (31), for the case that the convergence degree

β remains constant (= b^{-1} as for a purely exponential decrease), gives:

$$h = h_i \exp\left(\int -u_x \mathrm{D}t\right) \exp(\beta S) . \tag{32}$$

We introduce the auxiliary variable

$$h_p = h \exp(-\beta S) , \tag{33}$$

which represents the water depth compensated for the lateral compression due to width convergence. It then follows that the variation of the water depth due to the velocity gradient can be represented as

$$h_p = h_i \exp\left(\int -u_x \mathrm{D}t\right) . \tag{34}$$

This equation can be tested by means of the numerical model. The lateral compression due to the varying width can be removed, using numerical particle tracking for the particle displacement S. After applying Eq. (33), the transformed water depth h_p can be compared to the velocity u.

Lagrangean time series of h, h_p and u are plotted in Fig. 7 , together with the Lagrangean tidal ellipse in terms of horizontal and vertical displacements. It can be observed that there is a clear phase lag between h and u. However h_p has no phase lag with u, suggesting that h_p resembles a progressive wave. This resemblance is strongest in an "ideal" estuary, where convergence and friction are balanced so that there is no damping of the amplitude of the tidal wave. So an "apparently standing" wave in an "ideal" estuary (expressed in h and u) may also be described as a "progressive wave" (expressed in h_p and u) if we look at longitudinal compression only, as is the case in a prismatic channel where there is no lateral compression.

5.3 Classical vs. apparently standing waves

The open boundary Eq. (22) has been derived in Sect. 2.3 for a "perfect channel". However, if there is a closed boundary, then at this boundary the velocity will remain zero but the water level will change in time. Therefore neither invariant (see Eq. 6) will be constant in time at this location. Hence, it can be concluded that Eq. (22) cannot apply to a standing wave in a finite, frictionless, prismatic, horizontal channel.

Equation (22) does appear to hold in simulations of converging channels with open boundaries, as shown in Sect. 3, even though in these estuaries a clear phase lag can be observed. It does not hold in such converging estuaries if there is a closed boundary.

Since it appears to be the "classical reflection" which occurs at a closed boundary that causes Eq. (22) not to hold, it can be reasoned that if Eq. (22) does hold in converging estuaries with an open boundary, there is no such reflection. So the numerical results in Sect. 3 confirm that the phenomenon of "apparent reflection" (by convergence, friction and bed slope) is fundamentally different from "classical reflection" (by a closed boundary), as already noted in the literature (Hunt, 1964; Jay, 1991; Friedrichs and Aubrey, 1994; Toffolon and Savenije, 2011; Savenije, 2012).

6 Applications

6.1 Reconstructing the velocity

Through substitution of Eqs. (1) and (2) in Eq. (22), the spatial and temporal derivatives of the velocity can be removed, yielding a second order equation in u:

$$f_1 u^2 + f_2 u + f_3 = 0 \,, \tag{35}$$

where

$$f_1 = \zeta_x \, (h_x - \beta \, h \pm f_W \, h) \, ,$$
$$f_2 = h_t \, h_x + h_t \, \zeta_x - h_t \, \beta \, h \, ,$$
$$f_3 = h_t{}^2 - g \, h \, \zeta_x{}^2 \, ,$$
$$f_W = \frac{W}{u|u|} \, . \tag{36}$$

If convergence, friction and bed slope are known, Eq. (35) can be used to compute the velocity u directly out of observation of the water depth (h, h_t and h_x). But there are some issues that have to be addressed.

1. Observations cannot be completely local since spatial derivatives are required.

2. The specific friction term f_W has to be determined, which requires the local friction coefficient K to be estimated, or calibrated as discussed in Sect. 6.2. Here it is assumed that in open channels the full friction term W contains a quadratic velocity component, which is positive or negative depending on the flow direction.

3. Since this equation is of second order, it contains a part that can either be positive or negative, which changes within each simulation in a wave-like behavior.

Figure 8 illustrates the application of Eq. (35), in which the sign of the specific friction term $\pm f_W$ is taken from the numerical velocity and the sign of the quadratic root switches at the vertical asymptote. As can be observed, large spikes occur, which seem to introduce errors that dampen, but remain until the next spike.

Since numerical evaluations of the governing equations contain numerical errors, substitution may reduce or amplify the numerical error. Even though the proposed Eq. (35) is quite sensitive, in particular to small values of f_1, it is an interesting method to obtain the discharge flowing through the estuary from the easily observed water depth. In this sense, it functions as a stage-discharge method for the tidal zone.

Title Page

Abstract | Introduction

Conclusions | References

Tables | Figures

|◄ | ►|

◄ | ►

Back | Close

Full Screen / Esc

Printer-friendly Version

Interactive Discussion

6.2 Estimation of friction

A second application comes from removal of the spatial derivatives of both the water depth and the velocity, again through substitution, in order to determine the friction term W. Although the width convergence β and the bed slope Z_x cannot be measured locally, it is a large advantage of this method that only local time series are required of the water depth h and the velocity u. This can be done with

$$W = \frac{f_4 - f_5 f_6}{f_7}, \tag{37}$$

where

$$f_4 = g(h_t)^2 - h(u_t)^2, \quad f_5 = u(Z_x + \beta\, h),$$

$$f_6 = \left(\frac{u^2}{2} + g\, h\right)_t, \quad f_7 = (u\, h)_t. \tag{38}$$

A numerical test is shown in Fig. 9. The friction term W from Eq. (37) is compared to that obtained using Eq. (25) with three different values of the Strickler coefficient K. As the friction relates to the square of the velocity, the signal also shows pronounced spikes. The best agreement is found for $K = 50\,\mathrm{m}^{1/3}\,\mathrm{s}^{-1}$, which is the value used in the numerical simulation. Therefore Eq. (37) may be suitable for local friction calibration.

7 Summary and conclusions

An exact "open boundary equation" (Eq. 22) has been derived for a progressive wave in a frictionless, prismatic, horizontal and infinite channel, under sub-critical flow, which is valid in the entire modeling domain. It was further investigated through numerical simulations if this equation had more general validity in estuaries that experience convergence, friction and bed slope.

Numerical simulations with a weakly reflective boundary yielded satisfactory results for all amplitude-to-depth ratios, in weakly and in strongly converging estuaries, with low and high friction and with bed slope, as long as Eq. (22) was evaluated at sufficient distance from the imposed boundary conditions.

The additional equation is an integral part of the problem formulation, representing the information of the landward open boundary. In this way, the open boundary equation is an additional third equation to the two balance equations (Eqs. 1 and 2), providing limits to the solution space.

The open boundary equation does not work if there is "classical reflection" from a closed boundary. However, it does work if there is "apparent reflection" (by convergence, friction and bed slope), which is fundamentally different from "classical reflection".

The new equation can be used in practical applications, where it allows to remove two partial derivatives in the temporal and spatial variations of water elevation or velocity. In particular, removing the spatial derivatives of the velocity and water depth yields Eq. (27) for a fully absorbing, local boundary for the nonlinear Saint-Venant equations accounting for both friction and convergence. Alternatively, removing the velocity space and time derivative, Eq. (35) for the velocity u can be obtained from the water depth h and its derivatives in time h_t and space h_x. Moreover, Eq. (37) is found with which friction can be calibrated locally from time series observations of both velocity and water depth.

Although there are substantial hints that Eq. (22) is indeed valid for any infinite channel, also with friction and convergence, this cannot formally be proven yet. Numerical simulations contain errors and can only examine an intrinsically limited region of the parameter space on a finite domain, so we recommend that further research is performed on this approach to look for formal proof.

Appendix A: The open boundary equation in analytical approximations

In this section we consider some analytical approximations of progressive wave solutions (e.g., Savenije, 2012), to verify if Eq. (22) holds, and under which conditions. Ω and Ψ are any periodic function, η and υ are amplitudes of water level and velocity, φ is the variable part of the argument which is the same for ζ and u, ϵ is the phase lag.

A1 Progressive wave without damping

A progressive wave can be described by two generic periodic functions as

$$\zeta(x,t) = \eta\Psi(\varphi(x,t)), \tag{A1}$$
$$u(x,t) = \upsilon\Omega(\varphi(x,t)), \tag{A2}$$

whose partial derivatives are

$$\zeta_t = \eta\Psi_\varphi\varphi_t, \qquad \zeta_x = \eta\Psi_\varphi\varphi_x,$$
$$u_t = \upsilon\Omega_\varphi\varphi_t, \qquad u_x = \upsilon\Omega_\varphi\varphi_x. \tag{A3}$$

By multiplying the crossed partial derivatives it is straightforward to obtain that

$$\zeta_t u_x = u_t\zeta_x, \tag{A4}$$

thus demonstrating the validity of Eq. (22) in this case.

A2 Mixed wave with damping

In a damped wave, the amplitudes change along x. Considering a generic wave allowing for tidal damping/amplification, friction and convergence:

$$\zeta(x,t) = \eta(x)\Psi(\varphi(x,t) + \epsilon(x)), \tag{A5}$$
$$u(x,t) = \upsilon(x)\Omega(\varphi(x,t)). \tag{A6}$$

The derivatives now read

$$\zeta_t = \eta\Psi_\varphi\varphi_t, \qquad \zeta_x = \eta\Psi_\varphi(\varphi_x + \epsilon_x) + \eta_x\Psi,$$
$$u_t = \upsilon\Omega_\varphi\varphi_t, \qquad u_x = \upsilon\Omega_\varphi\varphi_x + \upsilon_x\Omega. \tag{A7}$$

Multiplying the derivatives as in Eq. (22) yields more complex results,

$$\zeta_t u_x = \eta\Psi_\varphi\varphi_t\upsilon\Omega_\varphi\varphi_x + \eta\Psi_\varphi\varphi_t\upsilon_x\Omega, \tag{A8}$$
$$u_t\zeta_x = \upsilon\Omega_\varphi\varphi_t\eta\Psi_\varphi(\varphi_x + \epsilon_x) + \upsilon\Omega_\varphi\varphi_t\eta_x\Psi. \tag{A9}$$

The validity of Eq. (22) in this case requires two conditions,

$$\epsilon_x = 0, \tag{A10}$$
$$\frac{1}{\eta}\eta_x\frac{1}{\Omega}\Omega_\varphi = \frac{1}{\upsilon}\upsilon_x\frac{1}{\Psi}\Psi_\varphi. \tag{A11}$$

The first condition (A10) is valid for a purely progressive wave ($\epsilon = 0$), but also for a mixed wave for which the phase between water level and velocity remains constant along x, which is the case in an ideal estuary but also in the asymptotic situation of alluvial estuaries (see Cai and Savenije, 2013)

The second condition requires more attention. If the structure of the two waves is characterized by a proportionality, i.e. $\Omega = k\Psi$, as it is often assumed, then Eq. (A11) becomes

$$\frac{1}{\eta}\eta_x = \frac{1}{\upsilon}\upsilon_x, \tag{A12}$$

which represents a requirement on the degree of damping of the velocity and water level amplitudes. In the case of linearized waves, this can be demonstrated to hold for infinitely long channels (Toffolon and Savenije, 2011), but the assumption of proportional damping (Eq. A12) is also at the basis of Savenije's approach (Savenije, 2012),

which has proved to yield satisfactory results for nonlinear cases (Cai et al., 2012, 2014). Finally, we note that a mixed wave in an ideal estuary clearly satisfies Eq. (22), since by definition in an ideal estuary the phase lag ϵ does not change (Eq. A10) and no damping is present (Eq. A11).

References

Cai, H. and Savenije, H. H. G.: Asymptotic behavior of tidal damping in alluvial estuaries, J. Geophys. Res.-Oceans, 118, 6107–6122, doi:10.1002/2013JC008772, 2013. 946

Cai, H., Savenije, H. H. G., and Toffolon, M.: A new analytical framework for assessing the effect of sea-level rise and dredging on tidal damping in estuaries, J. Geophys. Res.-Oceans, 117, C09023, doi:10.1029/2012JC008000, 2012. 947

Cai, H., Savenije, H. H. G., and Toffolon, M.: Linking the river to the estuary: influence of river discharge on tidal damping, Hydrol. Earth Syst. Sci., 18, 287–304, doi:10.5194/hess-18-287-2014, 2014. 947

De Saint-Venant, A. J. C. B.: Théorie du mouvement non permanent des eaux, avec application aux crues des rivières et à l'introduction de marées dans leurs lits, Comptes rendus des séances de l'Académie des Sciences, 73, 237–240, 1871. 926

Engquist, B. and Majda, A.: Absorbing boundary conditions for the numerical simulation of waves, Math. Comput., 31, 629–651, doi:10.1090/S0025-5718-1977-0436612-4, 1977. 927, 937

Friedrichs, C. T. and Aubrey, D. G.: Tidal propagation in strongly convergent channels, J. Geophys. Res.-Oceans, 99, 3321–3336, doi:10.1029/93JC03219, 1994. 926, 928, 941

Hunt, J. N.: Tidal oscillations in estuaries, Geophys. J. Roy. Astr. S., 8, 440–455, doi:10.1111/j.1365-246X.1964.tb03863.x, 1964. 926, 928, 941

Jay, D. A.: Green's law revisited: tidal long-wave propagation in channels with strong topography, J. Geophys. Res.-Oceans, 96, 20585–20598, doi:10.1029/91JC01633, 1991. 926, 928, 941

Keller, J. B. and Voli, D.: Exact non-reflecting boundary conditions, J. Comput. Phys., 82, 172–192, doi:10.1016/0021-9991(89)90041-7, 1989. 927, 937

Orlanski, I.: A simple boundary condition for unbounded hyperbolic flows, J. Comput. Phys., 21, 251–269, doi:10.1016/0021-9991(76)90023-1, 1976. 927

Riemann, G. F. B.: Über die Fortpflanzung ebener Luftwellen von endlicher Schwingungsweite, Abhandlungen der Königlichen Gesellschaft der Wissenschaften zu Göttingen, 8 , 43–65, 1859. 927

Savenije, H. H. G.: Lagrangian solution of St. Venant's equations for an alluvial estuary, J. Hydraul. Eng., 118, 1153–1163, doi:10.1061/(ASCE)0733-9429(1992)118:8(1153), 1992. 939

Savenije, H. H. G.: Salinity and Tides in Alluvial Estuaries, Elsevier, Amsterdam, 2005. 927

Savenije, H. H. G.: Salinity and Tides in Alluvial Estuaries, 2nd revised edn., available at: www.salinityandtides.com (last access: 26 May 2015), Delft, the Netherlands, 2012. 927, 933, 938, 941, 945, 946

Savenije, H. H. G., Toffolon, M., Haas, J., and Veling, E. J. M.: Analytical description of tidal dynamics in convergent estuaries, J. Geophys. Res.-Oceans, 113, C10025, doi:10.1029/2007JC004408, 2008. 928

Toffolon, M. and Savenije, H. H. G.: Revisiting linearized one-dimensional tidal propagation, J. Geophys. Res.-Oceans, 116, C07007, doi:10.1029/2010JC006616, 2011. 927, 937, 941, 946

Toffolon, M., Vignoli, G., and Tubino, M.: Relevant parameters and finite amplitude effects in estuarine hydrodynamics, J. Geophys. Res.-Oceans, 111, C10014, doi:10.1029/2005JC003104, 2006. 934, 936

Open boundary equation

D. Diederen et al.

Title Page

Abstract | Introduction

Conclusions | References

Tables | Figures

◄ | ►

◄ | ►

Back | Close

Full Screen / Esc

Printer-friendly Version

Interactive Discussion

Table 1. Parameter range for numerical simulations.

Parameter	Unit	Range
$\overline{h}_0$	m	2–40
α	–	0.01–0.6
γ_b	–	0–5|[a]
γ_d	–	0–0.5|[b]
K	$m^{1/3}\,s^{-1}$	20–80

[a,b] Approximately 15 % of the cases the value 0 is chosen.

Full Screen / Esc

Printer-friendly Version

Interactive Discussion
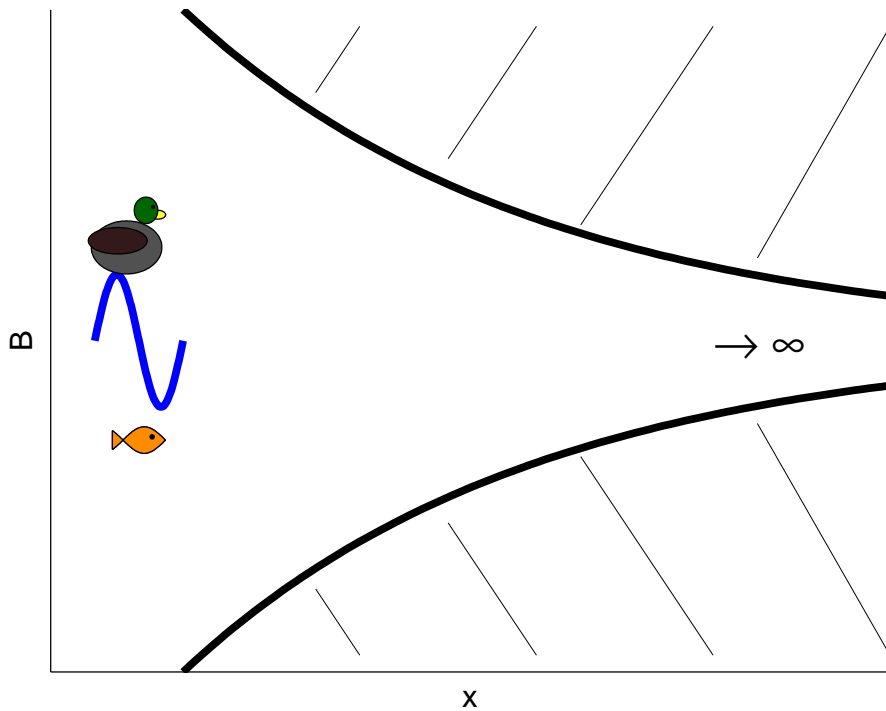
Figure 1. Tidal forcing in a converging channel of infinite length.

Back | Close

Full Screen / Esc

Printer-friendly Version

Interactive Discussion
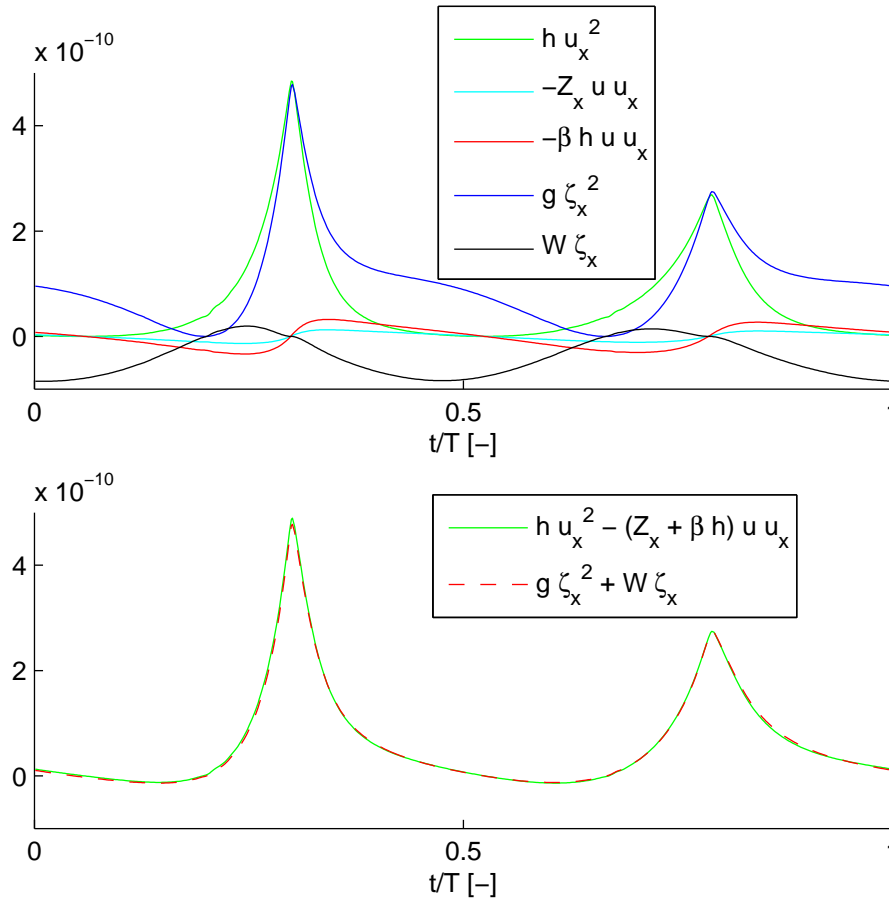
Figure 2. Time series are displayed of the terms in Eq. (26) at location $x = 0.2L$ for an estuary with $\eta = 0.1\,\text{m}$, $\bar{h}_0 = 10\,\text{m}$, $b = 70\,\text{km}$, $d = 200\,\text{km}$, $K = 45\,\text{m}^{1/3}\,\text{s}^{-1}$. In order to find good agreement between the left hand side and the right hand side, none of the terms can be neglected.
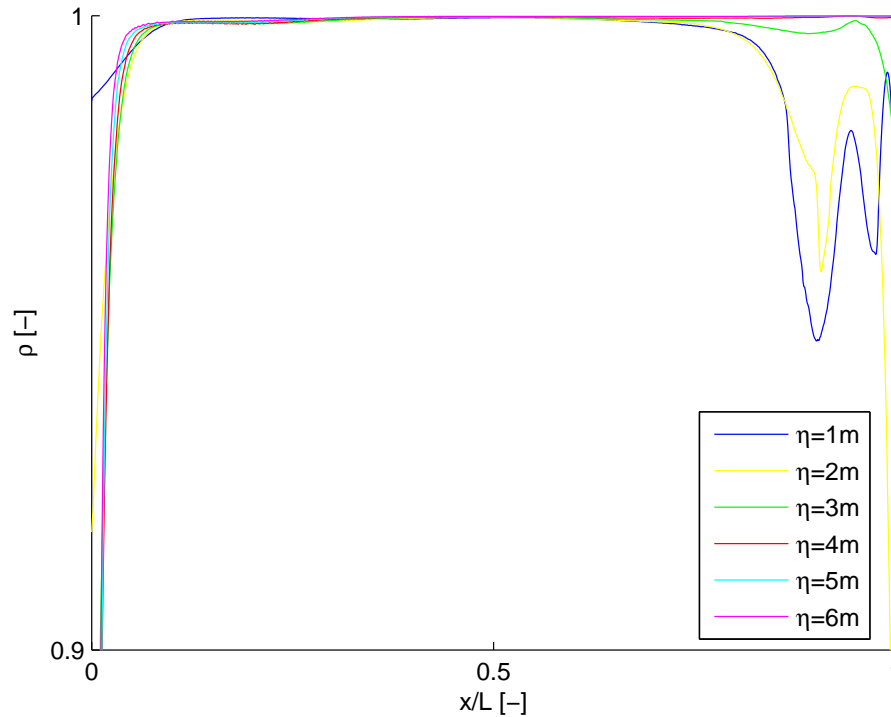
Figure 3. The Pearson coefficient ρ is displayed as a function of space, which correlates time series of the left hand side and the right hand side of Eq. (22) for an estuary with $\overline{h}_0 = 10\,\text{m}$, $b = 100\,\text{km}$, $d = 250\,\text{km}$, $K = 40\,\text{m}^{1/3}\,\text{s}^{-1}$, $L = 900\,\text{km}$ and a varying amplitude η.

Full Screen / Esc
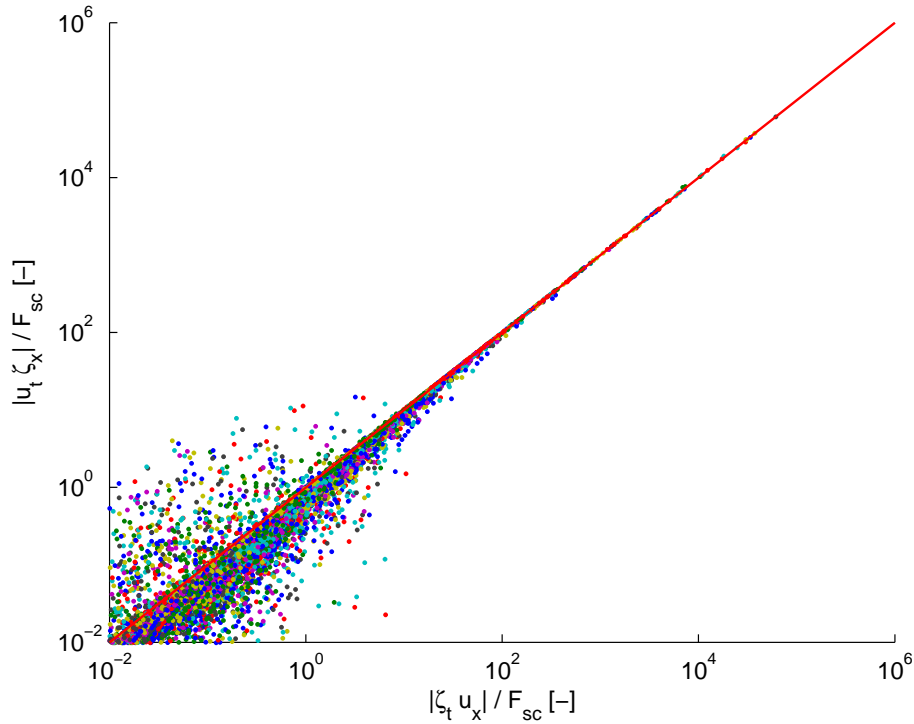
Figure 4. A parity diagram between absolute values of the scaled left hand side of Eq. (22) against the scaled right hand side, for 100 simulations in the range defined in Table 1. Each dot represents a time in the tidal cycle on a different location in the estuary domain $x = \{0.3L, 0.7L\}$.
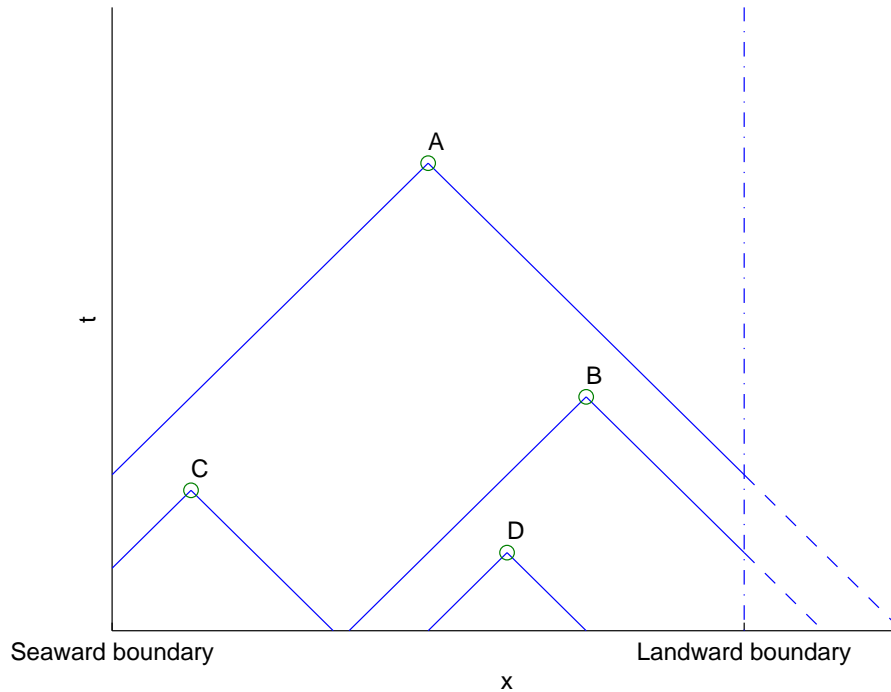
Figure 5. At each point (A, B, C, D) the solution for the water depth h and the velocity u depends on the values of both Riemann invariants. Each trajectory (which is implicitly dependent on the solution) leads back to an initial condition or a boundary condition.
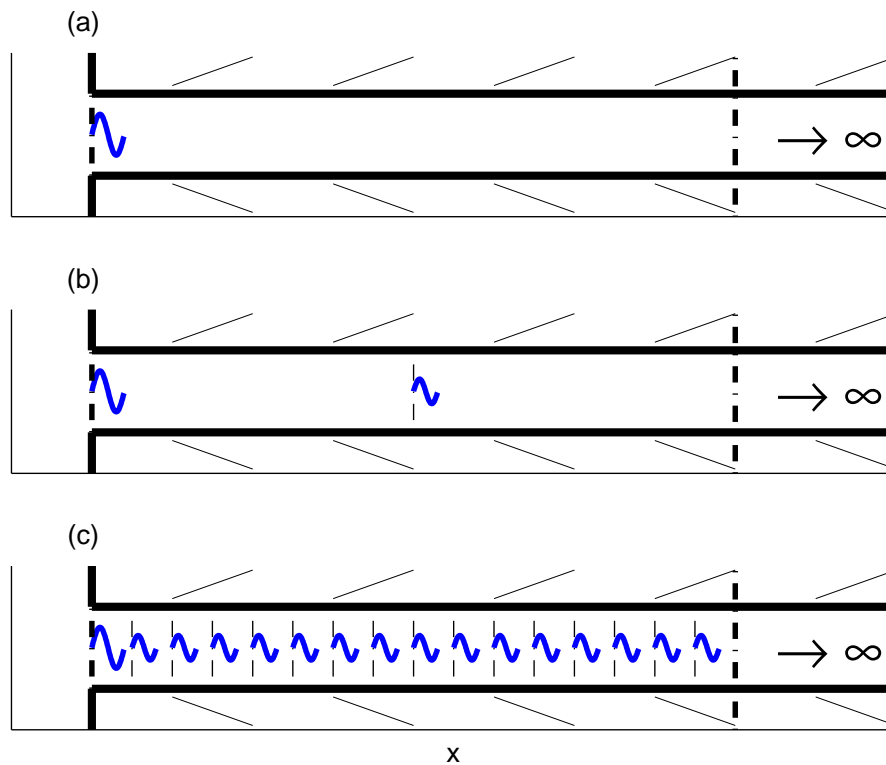
Figure 6. The same simulation is displayed on a domain with: **(a)** a single open boundary; **(b)** two open boundaries; or **(c)** a large number (theoretically infinite) of open boundaries.
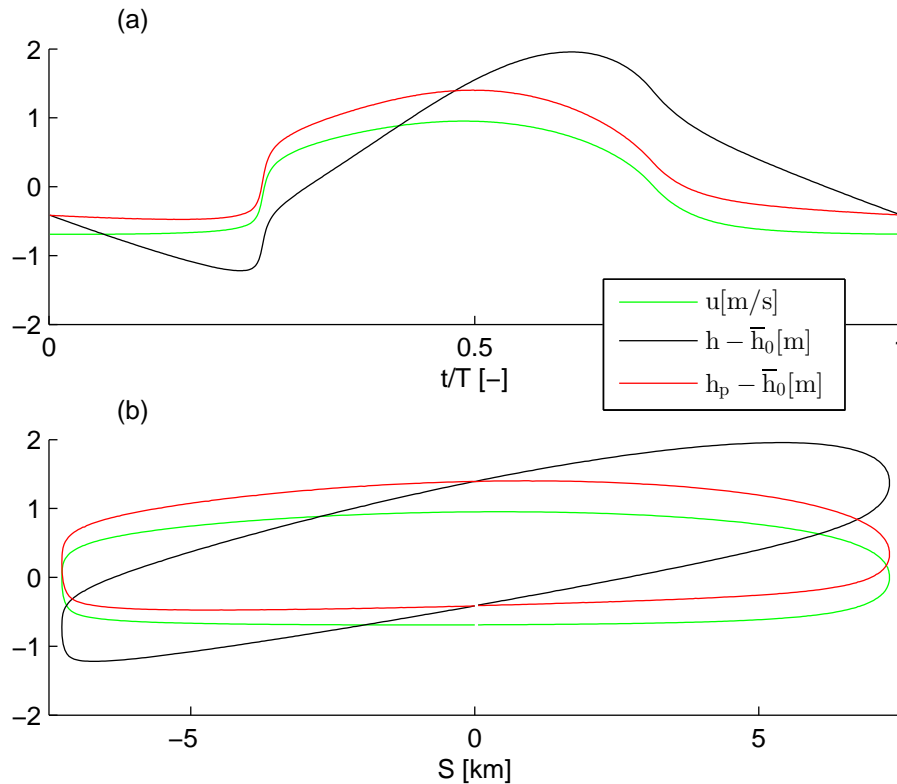
Figure 7. Decomposition of the vertical tide h separating the effect of convergence by introducing the variable h_p: **(a)** Lagrangean time series of h, h_p and velocity u; **(b)** the same variables as a function of the displacement. The used scenario is close to an ideal estuary, as $\eta = 2\,\text{m}$, $\overline{h}_0 = 10\,\text{m}$, $b = 70\,\text{km}$, $K = 45\,\text{m}^{1/3}\,\text{s}^{-1}$ and there is no bed slope.
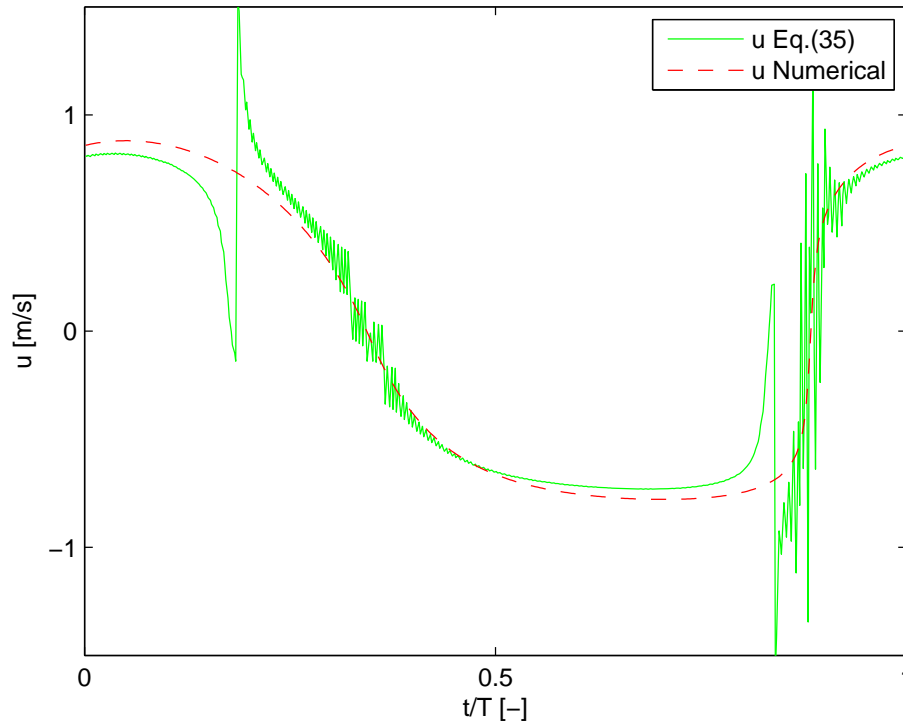
Figure 8. The resulting velocity from Eq. (35) is compared with the numerical velocity in time series. The parameters used in the simulation are $\eta = 1.2\,\text{m}$, $\overline{h}_0 = 28\,\text{m}$, $b = 280\,\text{km}$, $d = 1111\,\text{km}$, $K = 50\,\text{m}^{1/3}\,\text{s}^{-1}$.

Title Page

Abstract | Introduction

Conclusions | References

Tables | Figures

|◄ | ►|

◄ | ►

Back | Close

Full Screen / Esc

Printer-friendly Version

Interactive Discussion
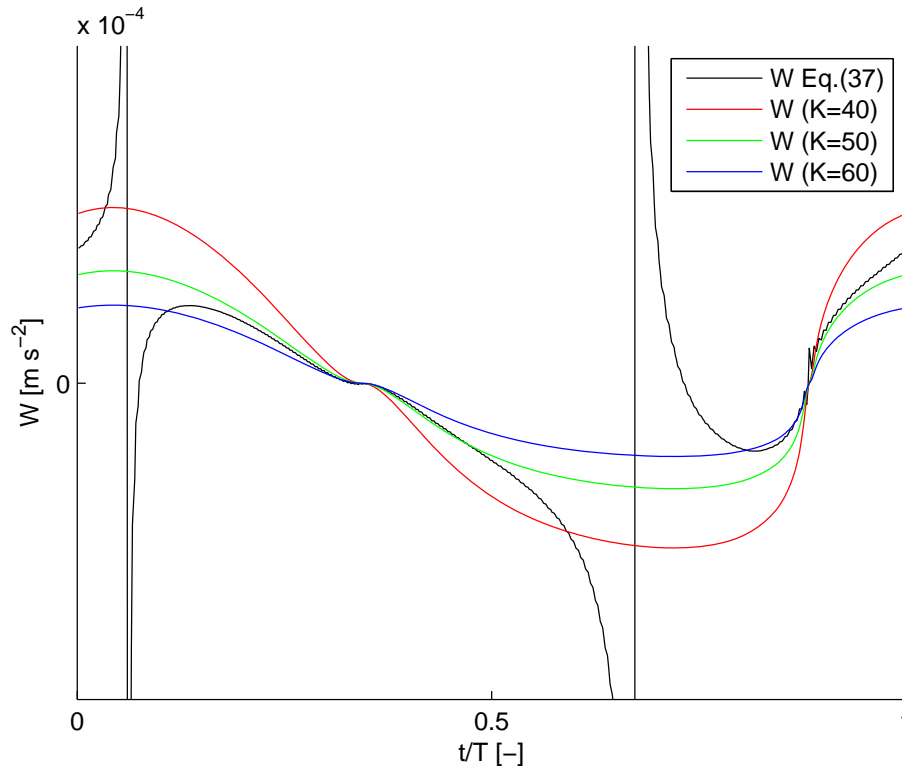
Figure 9. The result of Eq. (37) is compared with three estimates of the friction term W from Eq. (25), in which the numerical velocity has been used. The parameters are from the same simulation as in Fig. 8.